Integrated Simulations of Structural Performance, Molding Process, and Warpage for Gas-Assisted Injection-Molded Parts. III. Simulation of Cyclic, Transient Variations in Mold Wall Temperatures

SHIA-CHUNG CHEN, SHENG-YAN HU, WEN-REN JONG

Mechanical Engineering Department, Chung Yuan University, Chung-Li, Taiwan 32023, Republic of China

Received 9 March 1998; accepted 3 August 1998

ABSTRACT: Whether it is feasible to perform an integrated simulation for structural analysis, process simulation, as well as warpage calculation based on a unified CAE model for gas-assisted injection molding (GAIM) is a great concern. In the present study, numerical algorithms based on the same CAE model used for process simulation regarding filling and packing stages were developed to simulate the cooling phase of GAIM considering the influence of the cooling system. The cycle-averaged mold cavity surface temperature distribution within a steady cycle is first calculated based on a steady-state approach to count for overall heat balance using three-dimensional modified boundary element technique. The part temperature distribution and profiles, as well as the associated transient heat flux on plastic–mold interface, are then computed by a finite difference method in a decoupled manner. Finally, the difference between cycle-averaged heat flux and transient heat flux is analyzed to obtain the cyclic, transient mold cavity surface temperatures. The analysis results for GAIM plates with semicircular gas channel design are illustrated and discussed. It was found that the difference in cycle-averaged mold wall temperatures may be as high as 10°C and within a steady cycle, part temperatures may also vary ~ 15°C. The conversion of gas channel into equivalent circular pipe and further simplified to two-node elements using a line source approach not only affects the mold wall temperature calculation very slightly, but also reduces the computer time by 95%. This investigation indicates that it is feasible to achieve an integrated process simulation for GAIM under one CAE model, resulting in great computational efficiency for industrial application. © 1999 John Wiley & Sons, Inc. J Appl Polym Sci 71: 339–351, 1999

Key words: gas-assisted injection molding; gas channel; cyclic transient mold temperature; cycle-averaged BEM analysis; unified CAE model

INTRODUCTION

Gas-assisted injection molding (GAIM) process,[1–4] being an innovative injection molding process, can substantially reduce production expenses through reduction in material cost, reduction in clamp tonnage, and reduction in cycle time for thick parts. In addition, part qualities can also be greatly improved by reduction in residual stress, warpage, sink marks, and shrinkage. It also allows more design freedom in using structural ribs and bosses that would introduce sink mark and other associated issues on surface appearance when molded by conventional injection molding (CIM). Although gas-

Correspondence to: S.-C. Chen.

Journal of Applied Polymer Science, Vol. 71, 339–351 (1999)
 CCC 0021-8995/99/020339-13

assisted injection provides many advantages when compared with CIM, it also introduces new processing parameters in the process and makes the application more critical. One of the key factors is the design of gas channels that guide the gas flow to the desired locations. If the layout of gas channels and their corresponding dimensions and shapes in cross-sections are not properly designed, a catastrophe often occurred in the molded parts. In addition to the design parameters introduced by gas channels, other processing parameters—such as the numbers as well as the locations of gas injection points, amount of polymer melt injection, delay time, injected gas pressure, and holding time for gas injection, etc.—are also important in obtaining good molded parts. In another words, only when the design and processing parameters are well understood and GAIM process can obtain its advantage. Due to the complexity of gas channel design and processing control, computer simulation is expected to become an important and required tool to assist in part design, mold design, and process evaluation in the coming age. Fundamental studies concerning effect of gas channel design on gas penetration, molding window, as well as part properties, are also required to build quantitative design/molding guidelines that also help the application of GAIM.

At the present stage, process simulation for the melt filling and gas-assisted filling stages[3–8] has been developed, and some of them were incorporated into several commercial packages, such as C-GASFLOW, Moldflow/Gas, and CADMOLULD-MEGIT, etc. Two key factors that affect the simulation accuracy most are the algorithm used for the calculation of skin melt thickness and the geometrical modeling approach used to represent gas channels. The most popular modeling for gas channel is to use a circular pipe of equivalent hydraulic diameter and a superimposition approach[3,6–8] to represent the mixed one-dimensional and two-dimensional flow characteristics for melt and gas flow in the gas channel of noncircular cross-section. A schematic of such modeling is shown in Figure 1 for the semicircular gas channel. Such analysis approach has been verified for melt flow in thin cavity with channels of semicircular and quadrantal cross-sections reported recently.[7–9] Although the approach of assigning variable thickness to gas channels was used by CADMOLULD-MEGIT[4] and STRIMFLOW/Gas, it meets the difficulty for describing gas channels with a thin and long rib attached on their top. Basically, gas is not easy to penetrate this thin rib on the top of the gas channel. However, the assigning of a

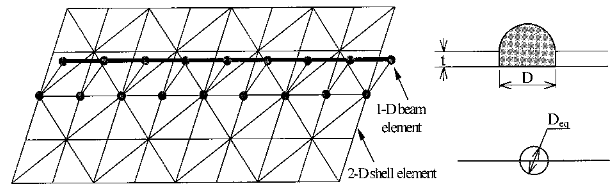

Equivalent Diameter : $D_{eq} = \sqrt{\dfrac{\pi D^2 + 8tD}{2\pi}}$

Shape Factor : $S.F. = \dfrac{D(1+\frac{\pi}{2})}{\pi D_{eq}}$

Figure 1 Schematic of the circular pipe to represent a semicircular gas channel. An equivalent diameter is calculated so that the melt flow area are the same for both models. 1-D, one-dimensional; 2-D, two-dimensional.

large thickness to a gas channel with a long tail rib may overpredict the gas penetration within this gas channel. Simulation results on the secondary gas penetration by both C-GASFLOW and Moldflow/gas show only very rough accuracy. A recent study[10,11] suggests that to obtain good simulation results for the secondary gas penetration in the gas-assisted packing stage, a new algorithm and a flow model of the shrinkage-induced origin may have to be introduced instead of just following the pressure-induced flow model used for the postfilling simulation of CIM.

Simulation of gas-assisted cooling is not available at this moment. Although the development for the simulation of gas-assisted cooling process is not too difficult, it does take the incorporation of geometry of the gas channels and the hollowed gas core into consideration. It is not known exactly how the geometrical simplification of a gas channel will affect the accuracy of cooling simulation. Generally speaking, a complete CAE package for the entire phase of the GAIM process is not available. On the other hand, a gas channel provides the capability of structural reinforcement and makes the reduction of part thickness possible. From the part designers' viewpoint, requirement in the evaluation of part structural performance and warpage become much more important in GAIM than that in conventional injection. Structural analysis for GAIM parts using three-dimensional analysis packages, such as ANSYS or ABAQUS, etc., are very time-consuming, especially when detailed geometry of the hollowed core caused by gas penetration was taken into consideration in the design/analysis stage. If warpage analysis also follows a three-dimensional analysis approach, it meets not only the

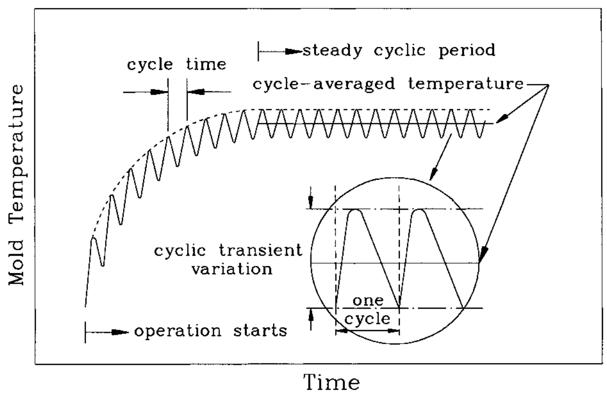

Figure 2 Schematic of cyclic, transient variation of the cooling process.

time-consuming issue but also the interface issue about how the results of process simulation conducted under 2.5-dimensional analysis characteristics can be transferred. Whether a unified finite element model can be used for process simulation (including melt filling, gas-assisted melt filling, and gas-assisted packing and cooling stages), structural analysis and warpage calculation are great concerns for CAE package development. In our previous studies,[7–11] simulations regarding primary gas penetrations within the filling stage and secondary gas penetration in the postfilling stage based on constant mold temperature have been reported. Structural analyses in the part design stage based on the same CAE finite model used for process simulation were also addressed and verified.[12–14] All previous process simulations developed by different groups assume constant mold wall temperatures. This is not true, as known by CIM. Particularly, contribution of thermal stress to the warpage formation will be even more significant than CIM, because GAIM requires much lower molding pressure, resulting in a lower flow-induced residual stress. In such a situation, accurate mold cavity surface temperature and part temperature distributions will be crucial to the thermally induced residual stress calculation. Gas penetration is very sensitive to melt temperature, mold temperature, cavity dimension accuracy, etc.. Small variation in these factors may result in uneven gas penetration for symmetrical gas channel design. As a result, only after a nonconstant mold temperature during the cooling phase of GAIM was obtained, the accurate prediction of gas penetration, as well as warpage, becomes possible for parts of complicated geometry. Basically, the cyclic cooling process (Fig. 2) in GAIM is a three-dimensional, time-dependent heat conduction problem with convective boundary conditions similar to that of CIM.[15–20] Complicated boundary geometry is introduced by the cooling channel and gas channel layout. Besides, there are many design parameters involved in the injection molding cooling process.[21] Although a complete analysis of the transient temperature variations of the mold and polymer melt simultaneously is possible in principle, the computational cost is too expensive to be implemented during the actual design process. To reduce the computing cost, a popular approach used by conventional injection mold cooling analysis is to use the boundary element method (BEM), in which the heat flux is introduced on the plastic–mold interface on a cycled-averaged basis[16–19] from which the cycle-averaged cavity surface temperatures can be obtained. Then, the transient variations of cavity surface temperature within a steady cycle were analyzed from the time-varying heat flux coming from each element representing local part thickness and melt temperature.

This article investigates the mold cooling stage simulation of GAIM, considering the influence from the mold cooling system so that the cyclic, transient variations of mold cavity surface temperatures, as well as part temperature distribution, can be calculated. Basically, the same approach used for cooling analysis in CIM was followed. Analyses were applied to the GAIM parts represented by a model with real semicircular gas channel geometry associated with a hollowed core (Fig. 3) and by the CAE model that converts the gas channel into an equivalent circular pipe with an exterior surface, as well as a line source ap-

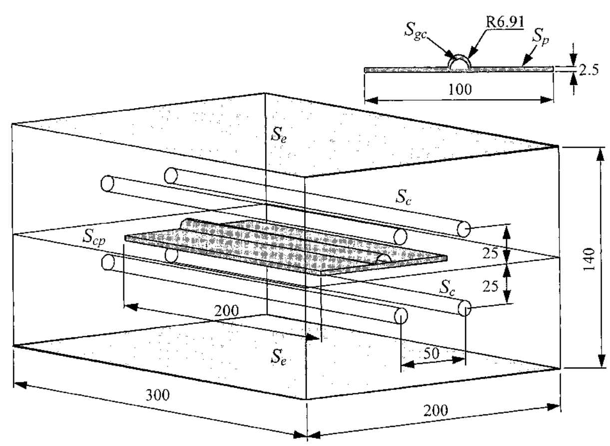

Figure 3 Geometric schematic of the GAIM plate part and mold.

proach model represented by the two-node element, respectively. The later approach is a common CAE model approach used for structural performance evaluation,[14] as well as simulations of melt filling and gas-assisted melt filling/holding phases.[3,6–11] Comparisons were also made to evaluate the differences in the predicted mold wall temperatures, as well as their cyclic, transient variations due to the gas channel conversion and simplification.

THEORETICAL FORMULATION

In previous studies,[15–19] the periodic transient mold temperature has been separated into two components: (1) a steady cycle-averaged component, $T_{m,s}$, and (2) a time-varying component, $T_{m,t}$, within a typical cycle, i.e.,

$$T_m(\vec{r}, t) = T_{m,s}(\vec{r}) + T_{m,t}(z, t) \qquad \text{for} \quad \vec{r} \in \Omega_m \quad (1)$$

The steady temperature component, $T_{m,s}$, is obtained by the cycle-averaged boundary element analysis. The temperature field in the mold is governed by a steady-state heat conduction equation of the Laplacian type:

$$\nabla^2 T_{m,s} = 0 \qquad \text{for} \quad \vec{r} \in \Omega_m \quad (2)$$

Corresponding boundary conditions defined over the boundary surface of the mold are described in the following:

$$-K_m \frac{\partial T_{m,s}}{\partial n} = h_{\text{air}}(T_{m,s} - T_{\text{air}}) \qquad \text{for} \quad \vec{r} \in S_e \quad (3)$$

$$-K_m \frac{\partial T_{m,s}}{\partial n} = h_c(T_{m,s} - T_{\text{air}}) \qquad \text{for} \quad \vec{r} \in S_c \quad (4)$$

$$-K_m \frac{\partial T_{m,s}}{\partial n} = \bar{q}_{cp} \qquad \text{for} \quad \vec{r} \in S_{cp} \quad (5)$$

$$-K_m \frac{\partial T_{m,s}}{\partial n} = \bar{J}_{av} \qquad \text{for} \quad \vec{r} \in S_p \quad (6)$$

where S_e, S_c, S_{cp}, S_p, and Ω_m represent the mold exterior surface, the cooling channel surface, the clamping surface, melt–mold interface, and the domain of the mold, respectively. The corresponding heat transfer coefficients for air and coolant are designated as h_{air} and h_c; $\bar{q}_{cp}$ is the heat flux value defined at the mold clamping surface; $\bar{J}_{av}$ is the cycle-averaged heat flux transferred from the polymer melt into the cavity surface and is defined as follows. The ambient environment temperatures, with respect to the mold, T_{air} and T_c, are defined for air and coolant correspondingly. K_m is the thermal conductivity of the mold. The cycle-averaged heat flux $\bar{J}_{av}$ is evaluated through numerical iterations. The time-varying component, $T_{m,t}$, within a typical cycle is approximated by one-dimensional transient heat conduction expressed as

$$\rho_m C_m \frac{\partial T_{m,t}(z, t)}{\partial t} = \frac{\partial}{\partial z}\left(K_m \frac{\partial T_{m,t}(z, t)}{\partial z}\right) \qquad \text{for} \quad z \in S_p \quad (7)$$

where ρ_m, C_m, and K_m are the density, specific heat, and thermal conductivity of the mold, respectively. Within the mold cavity, the polymer melt also satisfies the transient conduction equation of

$$\rho_p C_p \frac{\partial T_p}{\partial t} = \frac{\partial}{\partial z}\left(K_p \frac{\partial T_p}{\partial z}\right) \qquad \text{for} \quad \vec{r} \in \Omega_p \quad (8)$$

where ρ_p, C_p, K_p, and Ω_p are the density, specific heat, thermal conductivity, and domain of the polymer melt, respectively. On the mold cavity surface, S_p, compatible conditions must be fulfilled. That is,

$$K_m \frac{\partial T_m}{\partial n} = -K_p \frac{\partial T_p}{\partial n} \qquad \text{for} \quad \vec{r} \in S_p \quad (9)$$

$$T_m = T_p \qquad \text{for} \quad \vec{r} \in S_p \quad (10)$$

In addition, on the hollowed-core surface, S_{gc}, located within a gas channel, the boundary condition must satisfy

$$-K_p \frac{\partial T_p}{\partial n} = h_{N_2}(T_p - T_{N_2}) \qquad \text{for} \quad \vec{r} \in S_{gc} \quad (11)$$

where h_{N_2} and T_{N_2} are the heat transfer coefficient and the temperature of nitrogen injected during gas-assisted filling and packing phases, respectively. Along the mold cavity surface, it is subjected to a periodic boundary condition specified by the time-varying flux, $J_t = J(t) - \bar{J}_{av}$, at the cavity surface. During the analysis instant, t_i, the instantaneous heat flux $J(t_i)$ at the mold–

plastic interface is computed from the polymer melt temperature when the mold is closed. When the mold is open, a convective boundary condition similar to eq. (3) is defined for the cavity surface. The cycle-averaged heat flux $\bar{J}_{av}$ is then obtained by

$$\bar{J}_{av} = \frac{\Sigma J(t_i)\Delta t_i}{t_{\text{cycle}}} \tag{12}$$

where Δt_i is the interval between two computations and t_{cycle} is the cycle time. Analysis, as well as iteration algorithms, have been reported previously.[16–19]

In eq. (13), heat transfer coefficient, h_c, is calculated using the following Dittus–Boetler correlation[22] for internal forced convective heat transfer:

$$h_c = 0.023\,\frac{K_c}{D}\,\mathrm{Re}^{0.8}\,\mathrm{Pr}^{0.4} \tag{13}$$

where Re is the Reynolds number $= 4Q/\pi D\nu$ and Pr is the Prandtl number defined as ν/α. Here, Q denotes the volumetric flow rate; D is the diameter of the cooling channel; and ν is the kinematic viscosity of the coolant, with α and K_c being its thermal diffusivity and conductivity, respectively. This correlation is valid for $10{,}000 < \mathrm{Re} < 120{,}000$ and $0.7 < \mathrm{Pr} < 120$.

NUMERICAL METHODOLOGY

Numerical methods for steady-state boundary element analysis on a cycle-averaged basis have been reported previously.[16–19] The finite difference method for polymer melt heat transfer is also introduced with the same criteria for the adjustment of analysis interval.

The heat conduction eq. (2) is then transformed into an integral equation using Green's second identity, the fundamental solution technique,[23] and the fundamental solution of the Laplace equation:

$$C_i T_i = \int_\Gamma T^* q\, d\Gamma - \int_\Gamma q^* T\, d\Gamma \tag{14}$$

where T^* is $1/4\pi r$, q^* is $(\partial T^*/\partial n)$, and r is the distance between integral source point and field point. Equation (14) is a typical formulation used in the previous studies for part and mold represented by triangular elements for all related surface boundaries, Γ.

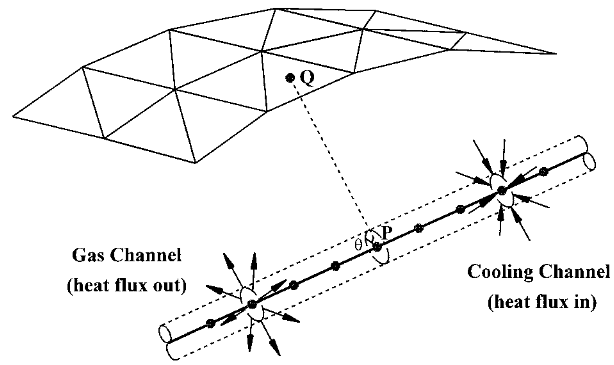

Figure 4 Schematic of the one-dimensional line source method to represent the circular cooling channels or gas channels.

To avoid discretization of the circular channel along the circumference that requires a lot of small triangular shell elements and thus saves a substantial amount of computer memory, the so-called line source (sink) approach first developed by Barone and Caulk[24] and further extended by Rezayat and Burton[25] for cooling channel simplification in three-dimensional parts was implemented. In this approach, the line source (sink) analog is applied to temperature and heat flux on each segment of the circular cooling channel. A schematic is shown in Figure 4. In such a situation, for the elements on the axis of the jth cylindrical segment of the cooling lines, eq. (14) can be further extended and expressed by[25]

$$\int_{l_j}\int_\Gamma (T^*q - q^*T)\, d\Gamma dl(P) + \int_{l_j}\sum_{j=1}^{N}\int_{e_j}(T^*q - q^*T)d\Gamma dl(P) = 0 \tag{15}$$

where P, l_j, and N are the source point on the axis of the jth cylindrical segment, the axis of the jth segment, and the total segment number of the cooling channels, respectively. Details have been reported.[24–26] In evaluation of the integrals over the cooling channel segments described herein, one can derive analytical expressions for integrals in θ direction for circular geometry and thus avoid the necessity of a mesh for cooling channels in the azimuthal direction.

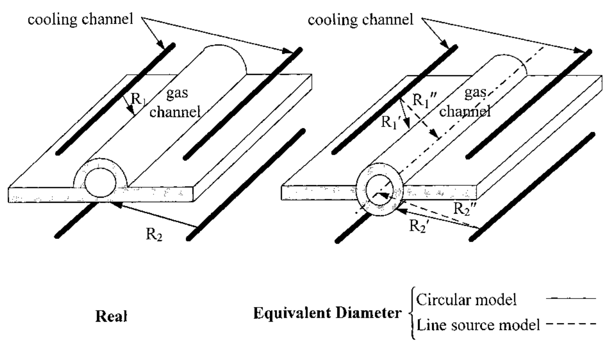

Figure 5 Variation of the cooling channel to gas channel distance due to the simplification of gas channel geometry.

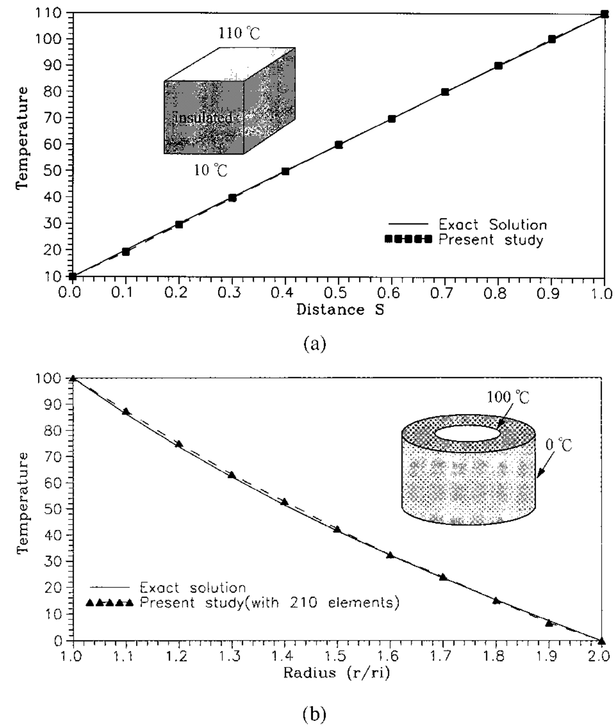

Figure 6 (a) Temperature distribution of a unit cube with two opposite sides maintained at temperatures of 10°C and 110°C, whereas all the other faces are insulated. Numerical results obtained from both BEM and analytical solution are demonstrated. (b) Temperature distribution of a hollow cylinder with both flat ends insulated and with the inner and outer lateral surfaces maintained at temperatures of 0°C and 100°C, respectively. Numerical results obtained from both BEM and analytical solution are demonstrated.

Similarly, the method described herein can be also applied to a gas channel represented by two-node elements attributed with equivalent diameters. However, the gas channel behaves like a heat source, in contrast with the heat sink behavior of cooling channels (Fig. 5). The residual wall thickness (resulting from gas penetration) of the gas channel must be included for heat flux calculation. This approach not only minimizes the using of tiny triangular elements on the cooling channel surfaces, as well as the outer gas channel surfaces, but also avoids the aspect ratios issue[27] that will increase the large number of triangular elements required for the mold exterior surface during analysis, considering the numerical stability.

Because the constant planar triangular element is implemented in this formulation, $C = 1/2$ for boundary points. The detail mathematical procedure for this direct formulation technique are described elsewhere.[16–19] After discretization over the boundary, eq. (3) can be discretized into a set of linear equations

$$[H]\{T\} = [G]\{q\} \tag{16}$$

where $\{T\}$ and $\{q\}$ represent column matrices for temperature and heat flux, respectively. By introducing the boundary values, eq. (16) can be rearranged to be in the form of

$$[A]\{T\} = \{B\} \tag{17}$$

Table I Material Properties and Processing Parameters

1. Thermal properties of polymer melt and mold:
   $K_p = 0.15$ W m^{-1} K^{-1}, $C_p = 2.1$ kJ kg^{-1} K^{-1}, and $\rho = 1{,}040$ kg m^{-3}
   $K_m = 36.5$ W m^{-1} K^{-1}, $C_m = 0.46$ kJ kg^{-1} K^{-1}, and $\rho_m = 7{,}820$ kg m^{-3}
2. Flow rate of coolant: 10 L min^{-1} Diameter of cooling channel: 10 mm
3. Ambient air temperature: 25°C Heat transfer coefficient of air: 10 W m^{-2} K^{-1}
4. Nitrogen temperature: 25°C Heat transfer coefficient of nitrogen: 10 W m^{-2} K^{-1}
5. Thickness of plate for the GAIM part: 2.5 mm
6. Initial polymer melt temperature: 230°C
7. Mold open time: 5 s

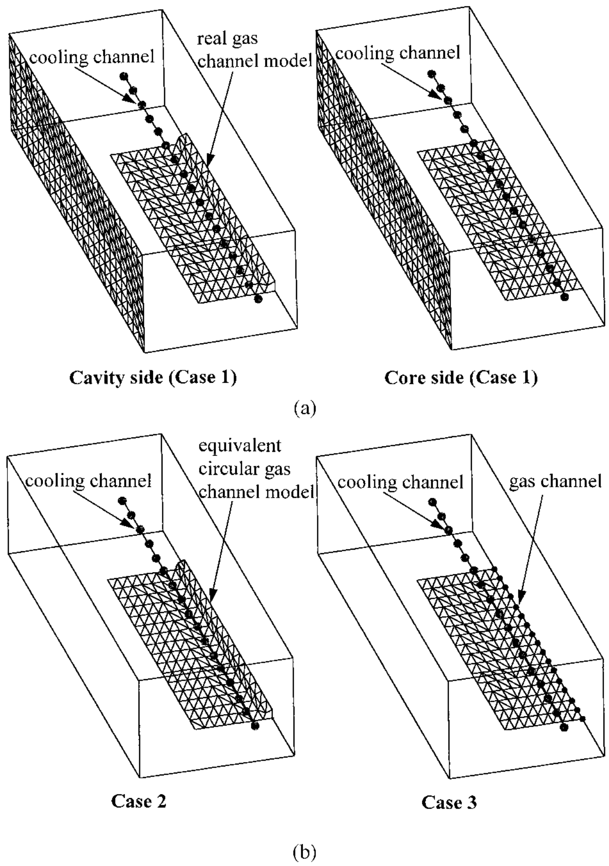

Figure 7 (a) BEM mesh model for mold exterior surface, cooling channel as well as part. Gas channel is modeled according to real geometry (case 1). Mesh models for both core side and cavity side are required due to the asymmetry of the gas channel geometry. (b) BEM mesh model for mold exterior surface, cooling channel as well as part. Gas channels are modeled by two methods. One is an equivalent circular gas channel required triangular elements meshed along its exterior surface (case 2). The other is a two-node element (line source model) representation similar to cooling channel (line sink model) (case 3).

Solving eq. (17), the cycle-averaged mold wall temperatures, including plastic-mold interface temperature, are obtained. The mold cavity surface temperatures are then used to compute the polymer melt temperature profile and distribution by eq. (8). Equation (8) is solved by the finite difference method. For gas channel, the heat conduction equation for the hollowed cylinder must be used, discretized, and solved.

To test the numerical accuracy of the presently developed BEM software, a unit cube with two opposite sides maintained at temperatures of 10°C and 110°C, all of the other faces insulated are used first. The exact solution for this is simply a linear variation with the coordinate in the direction along which temperature varies from 10°C to 110°C. From Figure 6(a), it can be seen that the comparison between the simulated values and those obtained from the exact solution are coincidental. In the second case, a hollow cylinder had both flat ends insulated and the inner and outer lateral surfaces maintained at temperatures of 0°C and 100°C, respectively. The exact solution for the temperature in this case is simply a logarithmic variation with the radius. In Figure 6(b), one can also see the numerical prediction showing good consistency, compared with the exact solution.

SIMULATED RESULTS AND DISCUSSIONS

During the simulations, all the material properties and the cooling operation conditions are listed in Table I. A plate part designed with a gas channel of semicircular cross-section was used as the analysis case. Three BEM models of plate parts with real semicircular gas channel geometry (case 1) [as shown in Fig. 7(a)] and with an equivalent gas channel approach represented by a circular gas channel [Fig. 7(b)] meshed with triangular elements along the channel surface (case 2) and by a two-node element [Fig. 7(b)] similar to that of the cooling channel (case 3),

Table II Cooling Conditions of Simulated Cases

	Cooling Time (s)	Coolant Temperature (°C)	Gas Channel Type (real/equivalent)
Case 1A	35	40	Real
Case 2A	35	40	Equivalent (circular model)
Case 3A	35	40	Equivalent (line source model)
Case 1B	45	60	Real
Case 2B	45	60	Equivalent (circular model)
Case 3B	45	60	Equivalent (line source model)

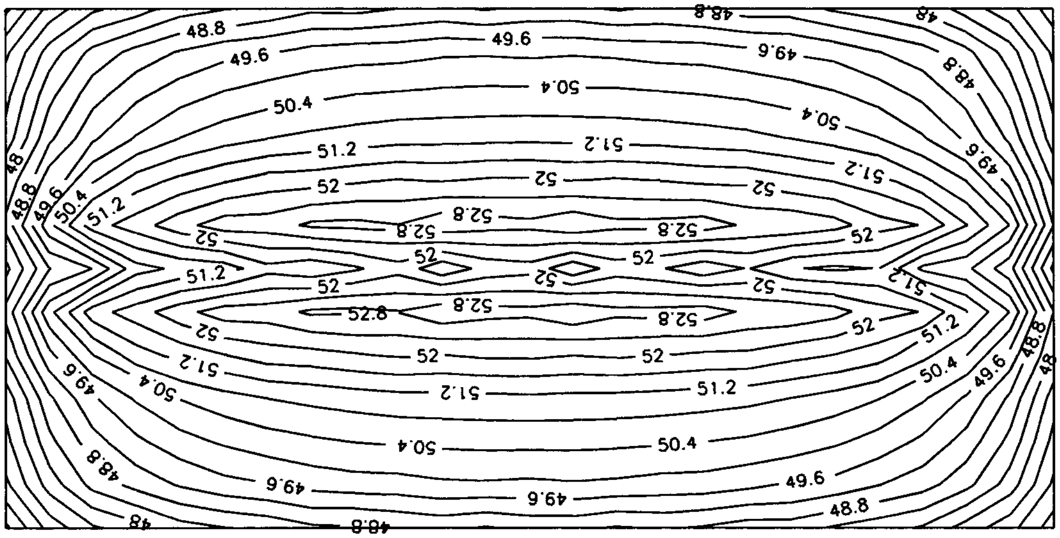
48
48.8
49.6
50.4
51.2
52
52.8

(a)

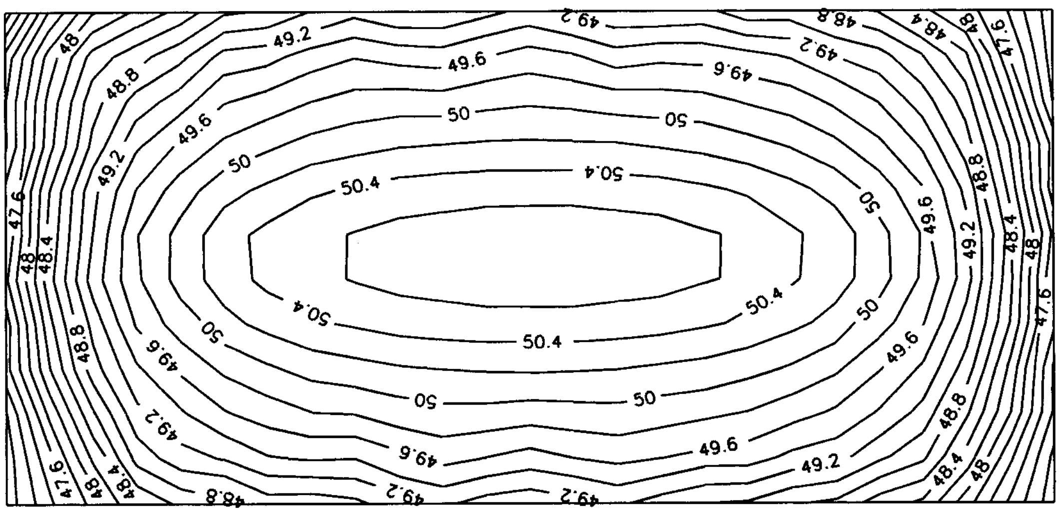
47.6
48
48.4
48.8
49.2
49.6
50
50.4

(b)

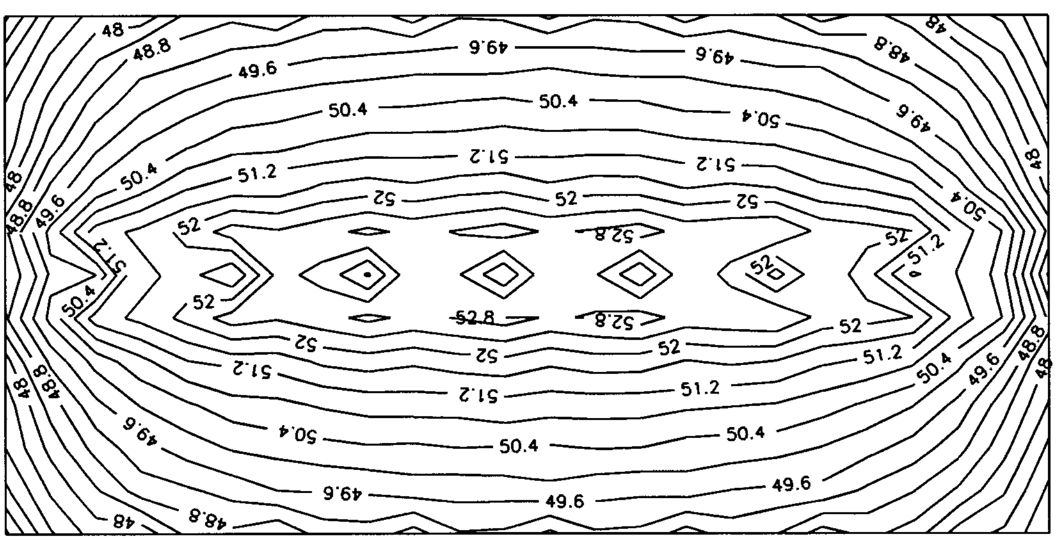
48
48.8
49.6
50.4
51.2
52
52.8

(c)

Figure 8

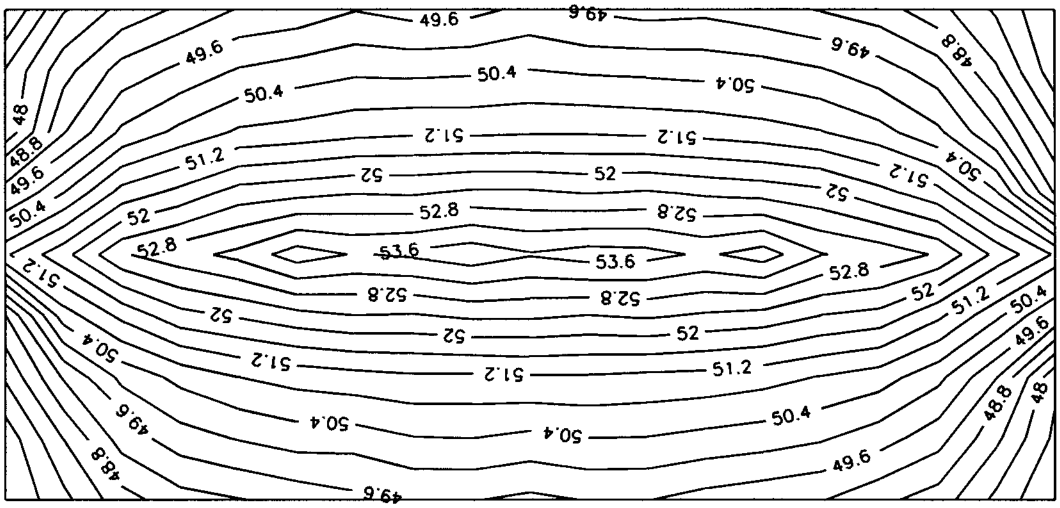

(d)

Figure 8 (*Continued from the previous page*) (a) Cycle-averaged mold wall temperature distribution of the cavity side for the GAIM part with real semicircular gas channel modeling (case 1A). (b) Cycle-averaged mold wall temperature distribution of the core side for the GAIM part with real semicircular gas channel modeling (case 1A). (c) Cycle-averaged mold wall temperature distribution of cavity or core side for the GAIM part with the gas channel approximated by an equivalent circular gas channel (case 2A). (d) Cycle-averaged mold wall temperature distribution of cavity or core side for the GAIM part using a one-dimensional two-node element to represent the real gas channel (case 3A).

respectively, were used. For each case, two different coolant temperatures and cooling times were assumed (as displayed in Table II). Due to the gas channel conversion, the distances from gas channel surface to cooling channels may be varied. Basically, triangular elements were implemented on the mold exterior surface, parting surface, part surface (cavity surface), and the surface of a gas channel with real semicircular geometry or equivalent circular geometry (cases 1 and 2). The cooling channel mesh was also reduced and represented by a two-node element. Due to the small triangular elements required for the gas channel surface and the associated aspect ratio issue, the total number of triangular elements during analyses for cases 1 and 2 are 4,808 and 2,404, respectively. For case 3, the required number of triangular element is 156 plus 12 two-node elements for the gas channel. For all cases, each cooling channel needs 16 two-node elements. Because of the asymmetry of the gas channel shape, both core side and cavity side must be included in the BEM model for case 1.

Simulated cycle-averaged mold cavity surface temperature distribution of the cavity side for the GAIM plate with a real semicircular gas channel geometry modeling (case 1A) is depicted in Figure 8(a). Maximum temperatures are around the gas channel laid-out locations. Also, around the plate center, the distance is farther away from the mold exterior surface. Therefore, the mold temperatures show the highest values. Cycle-averaged cavity surface temperature distribution of core side (case 1A) is shown in Figure 8(b). For GAIM plate with equivalent circular gas channel geometry modeling (case 2A), calculated cycle-averaged cavity surface temperature distribution is displayed in Figure 8(c). In case 3A, with the gas channel modeled by two-node elements, the predicted cycle-averaged cavity surface temperature distribution is illustrated in Figure 8(d). When different cooling conditions were assumed, the corresponding cavity surface temperature distribution on a cycle-averaged base are shown in Figure 9(a–d, respectively). The maximum and minimum values of the predicted temperatures are listed in Table III. Due to the influence of the cooling system and mold configuration, the cycle-averaged mold wall temperatures may differ by 10°C, even though the cooling channel design is symmetrical for both core side and cavity side. The influence of cooling system on mold wall temperatures should not be neglected. It can be noted that,

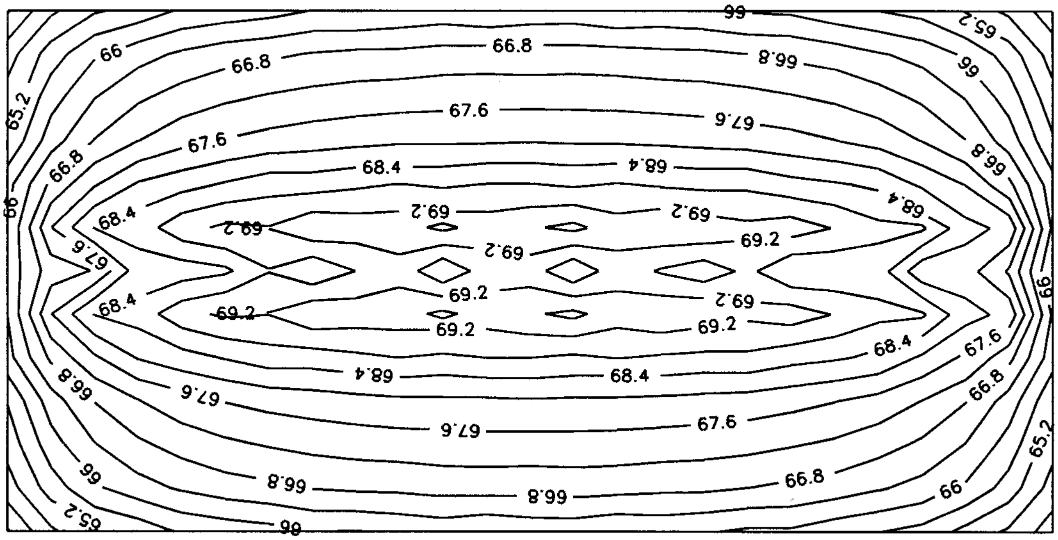
66
65.2
66.8
67.6
68.4
69.2

(a)

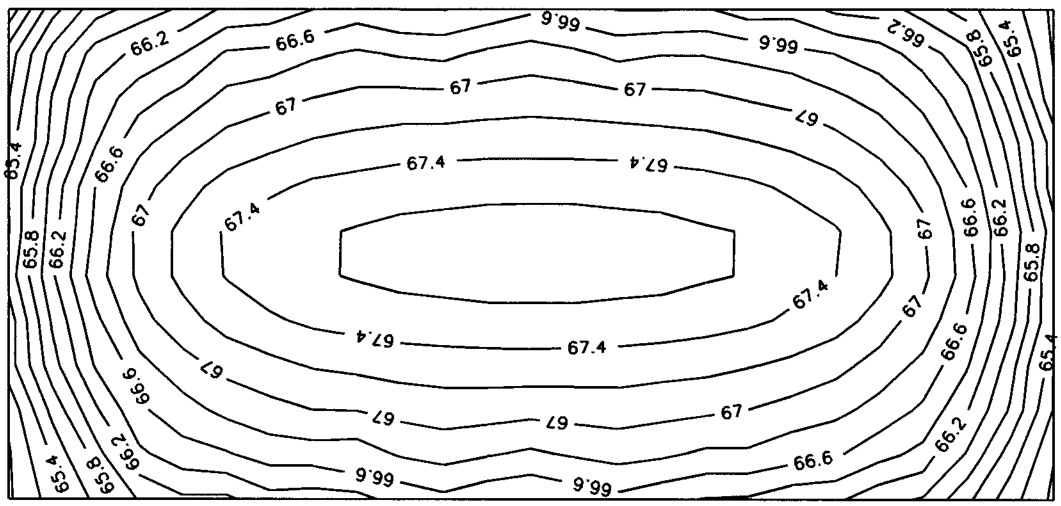
65.4
65.8
66.2
66.6
67
67.4

(b)

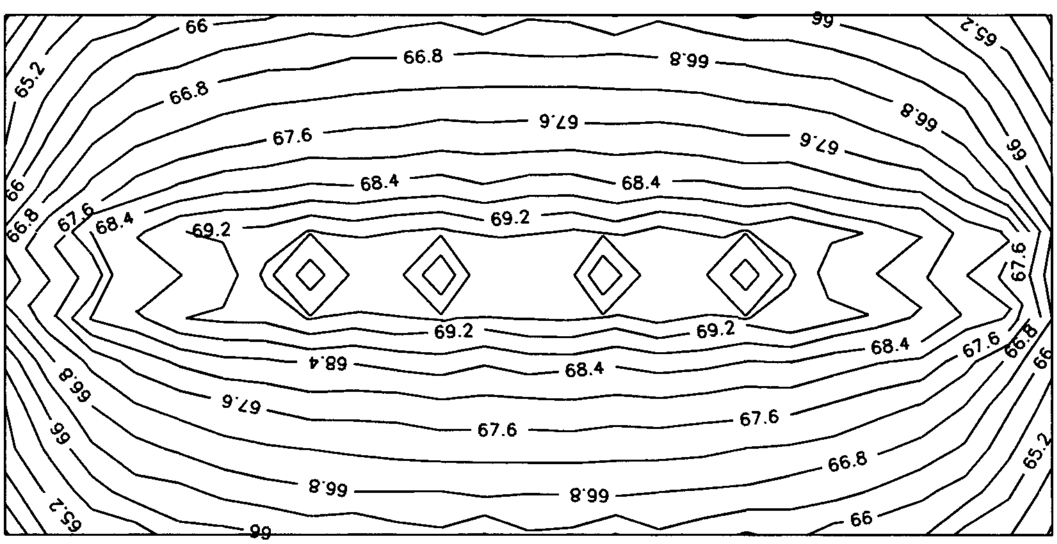
66
65.2
66.8
67.6
68.4
69.2

(c)

Figure 9

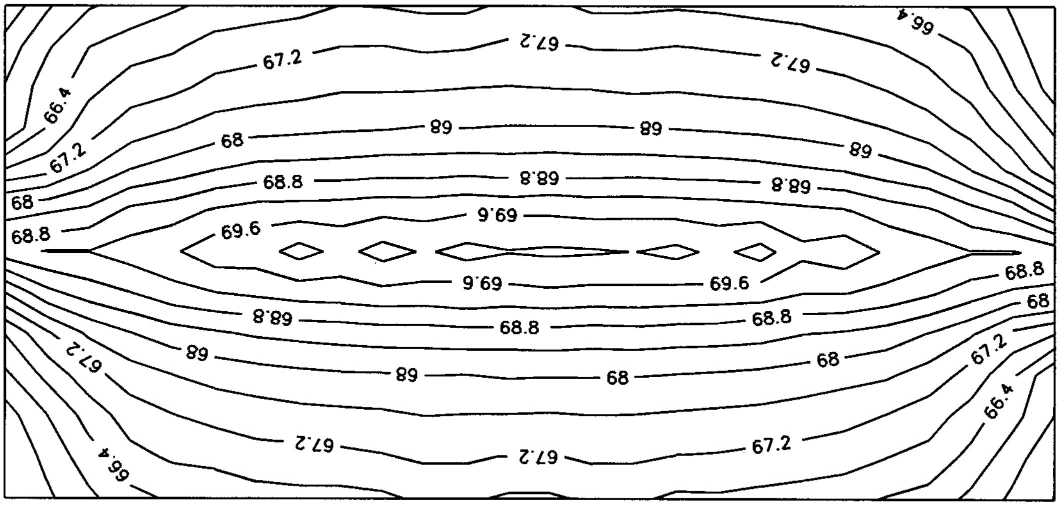

(d)

Figure 9 (*Continued from the previous page*) (a) Cycle-averaged mold wall temperature distribution of the cavity side for the GAIM part with real semicircular gas channel modeling (case 1B). (b) Cycle-averaged mold wall temperature distribution of the core side for the GAIM part with real semicircular gas channel modeling (case 1B). (c) Cycle-averaged mold wall temperature distribution of cavity or core side for the GAIM part with gas channel approximated by an equivalent circular channel (case 2B). (d) Cycle-averaged mold wall temperature distribution of cavity or core side for the GAIM part using a one-dimensional two-node element to represent the real gas channel (case 3B).

on the cavity side, the differences in these predicted temperatures using three models are only ~ 1°C. On the core sides, predicted values of case 1 are lower than others by ~ 4°C. However, the computer time has been reduced to only ~ 50% in case 2 and 5% in case 3, compared with case 1. This does not include the additional time to rebuild the gas channel surface and mesh model required for analyses. The calculated cyclic, transient variations of cavity wall temperatures at different locations on the plate and gas channel for all three cases with cooling condition A are also shown in Figure 10(a–c). It is also clear that, within a steady cycle, part temperatures may vary as high as 15°C. Comparison of cyclic, transient cavity wall temperatures at two gas channel locations designated as G1 and G3 are given in Figure 11(a,b). All three BEM models result in predicted values of <3%. This indicates that the current CAE model used for the simulations of filling and packing phases can be used also for cooling simulation. The cooling channel mesh (two-node elements), as well as the mold exterior mesh, must be added to account for the influence of the mold cooling system.

Table III Maximum and Minimum Cycle-Averaged Mold Cavity Temperature

	Maximum/Minimum (cavity side)	Maximum/Minimum (core side)
Case 1A	53.24°C/45.90°C	50.73°C/46.48°C
Case 2A	54.26°C/45.85°C	54.26°C/45.85°C
Case 3A	54.05°C/46.77°C	54.05°C/46.77°C
Case 1B	69.96°C/63.96°C	67.70°C/64.67°C
Case 2B	71.47°C/63.91°C	71.47°C/63.91°C
Case 3B	70.30°C/64.89°C	70.30°C/64.89°C

CONCLUSIONS

This study investigates that, whether it is feasible to perform an integrated simulation for structural analysis, process simulation (as well as warpage calculation) is based on a unified CAE model for GAIM, particularly, the modeling issue related to cooling phase simulation. Numerical algorithms based on the same finite element mesh used for process simulation regarding melt filling, gas-assisted melt filling, and gas-assisted packing stages were developed to simulate the cooling phase of GAIM using a three-dimensional modified boundary element technique. The cycle-averaged mold cavity surface temperature distribution within a

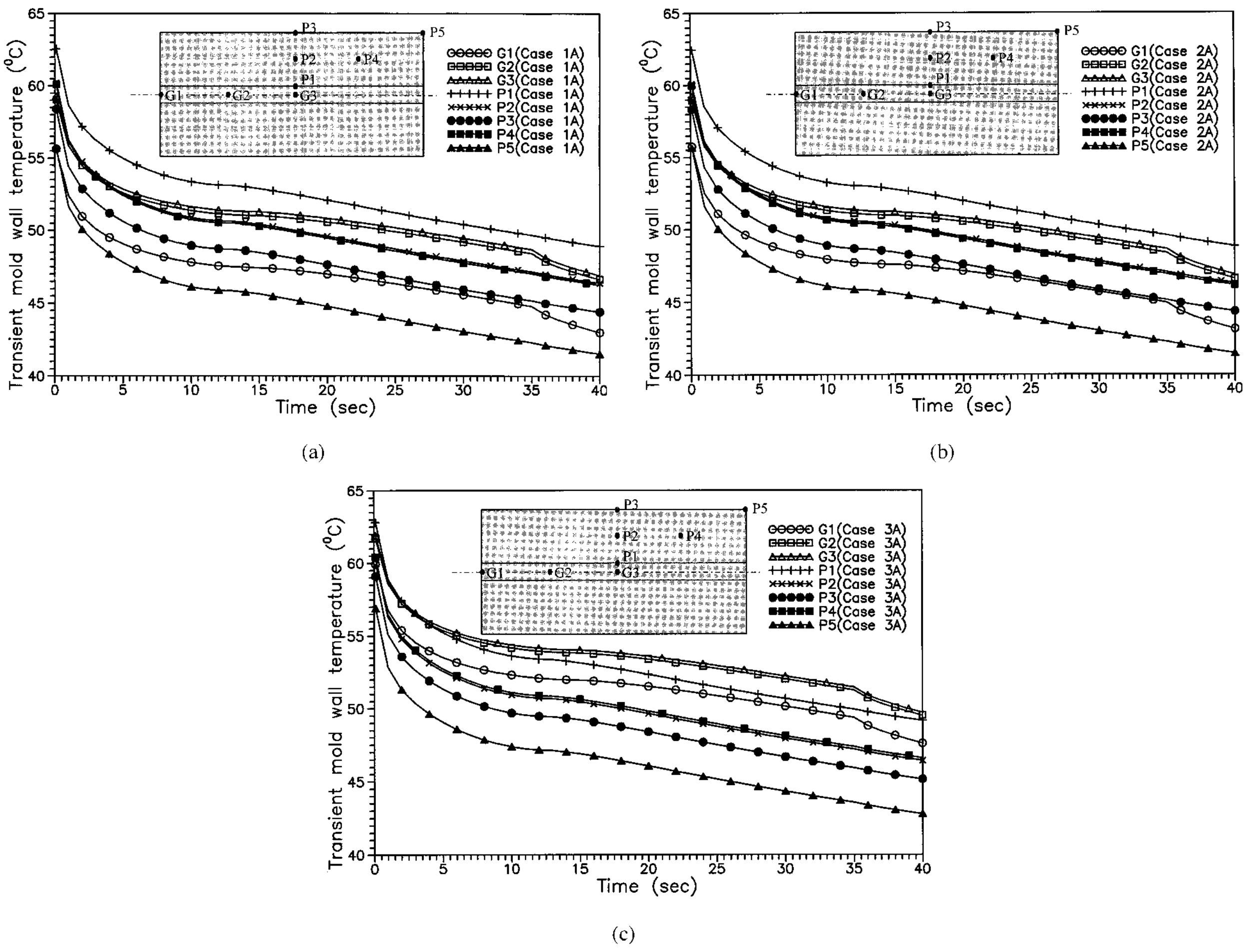

Figure 10 (a) Variations of cyclic, transient mold wall temperatures for case 1A at different gas channel locations designed as G1, G2, and G3, and part locations labeled as P1, P2, P3, P4, and P5. (b) Variations of cyclic, transient mold wall temperatures for case 2A at different gas channel locations designed as G1, G2, and G3, and part locations labeled as P1, P2, P3, P4, and P5. (c) Variations of cyclic, transient mold wall temperatures for case 3A at different gas channel locations designed as G1, G2, and G3, and part locations labeled as P1, P2, P3, P4, and P5.

steady cycle is first calculated based on a steady-state approach to account for overall mold heat balance. The part temperature distribution and profiles, as well as the associated transient heat flux on the plastic–mold interface, are then computed by the finite difference method in a decoupled manner. Finally, the difference between cycle-averaged heat flux and transient heat flux is analyzed to obtain the cyclic, transient mold cavity surface temperatures. Three BEM models, including real gas channel surface and equivalent circular gas channel surface meshed with triangular elements (as well as equivalent circular gas channel represented by two-node elements using a line source approach) were all analyzed. The following observations were found:

1. Cycle-averaged mold wall temperatures may differ by 10°C because of the influence of cooling system configuration, even under symmetrical cooling channel design on the core and cavity sides. Part temperatures may also vary $\sim$ 15°C within a steady cycle. Nonconstant mold wall temperatures should be considered for an accurate simulation.
2. The CAE model of real gas channel geometry requires about twice degree of freedom and CPU time, compared with the CAE model defined by an equivalent circular gas channel. However, when the gas channel is further converted into the two-node element model based on the line source ap-

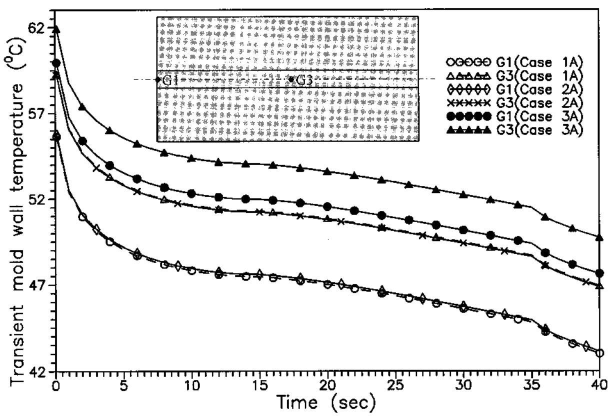

(a)

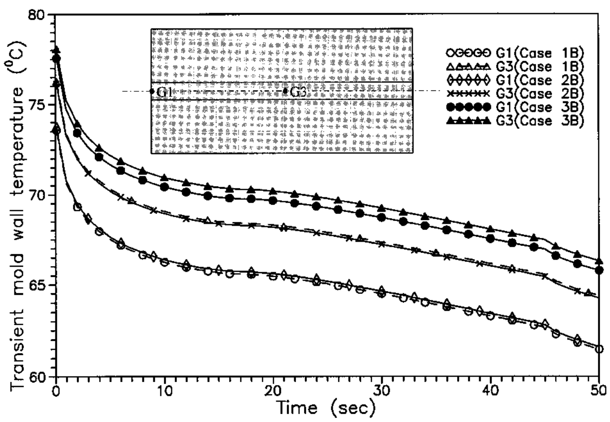

(b)

Figure 11 (a) Comparison of cyclic, transient mold wall temperatures for case 1A, case 2A, and case 3A at different gas channel locations designed as G1 and G3. (b) Comparison of cyclic, transient mold wall temperatures for case 1B, case 2B, and case 3B at different gas channel locations designed as G1 and G3.

proach, the degree of freedom has been reduced to ~ 30%, and CPU time becomes 5% of the original real gas channel model.

3. The differences in maximum and minimum cycle-averaged temperatures on the cavity side in all three analysis models are only ~ 1°C. One the core side, the differences may go up to ~ 4°C. All three BEM models result in predicted values in cyclic, transient temperatures of gas channel by < 3%.
4. This investigation indicates that it is feasible to achieve an integrated process simulation for the GAIM process under one CAE model resulting in great computational efficiency for industrial application.

This work was supported by the National Science Council under NSC Grant 87-2216-E033-007 and by Chung Yuan University under distinguished research funding.

REFERENCES

1. Rush, K. C. Plast Eng 1989, July, 35.
2. Shah, S. SPE Tech Paper 1991, 37, 1494.
3. Turng, L. S. SPE Tech Paper 1992, 38, 452.
4. Shah, S.; Hlavaty, D. SPE Tech Paper 1991, 37, 1479.
5. Lanvers, A.; Michaeli, W. SPE Tech Paper 1992, 38, 1796.
6. Sherbelis, G. SPE Tech Paper 1994, 40, 411.
7. Chen, S. C.; Cheng, N. T.; Hsu, K. S. Int J Mech Sci 1996, 39, 335.
8. Chen, S. C.; Hsu, K. F.; Hsu, K. S. Int J Heat Mass Transfer 1996, 39, 2957.
9. Chen, S. C.; Hsu, K. F. Numer Heat Transfer, Part A 1995, 28, 121.
10. Chen, S. C.; Cheng, N. T.; Hsu, K. S. Int Commun Heat Mass Transfer 1995, 22, 319.
11. Chen, S. C.; Cheng, N. T.; Hu, S. Y. J Appl Polym Sci 1998, 67, 1553.
12. Hu, S. Y.; Chien, R. D.; Chen, S. C.; Kang, Y. Plast Rubber Compos Pro 1997, 26, 172.
13. Chen, S. C.; Hu, S. Y.; Chien, R. D.; Huang, J. S. Polym Eng Sci 1998, 38, 1085.
14. Chen, S. C.; Hu, S. Y.; Chien, R. D.; Huang, J. S. J Appl Polym Sci 1998, 68, 417.
15. Austin, C. SPE Tech Paper 1985, 31, 764.
16. Kwon, T. H.; Shen, S. F.; Wang, K. K. SPE Tech Paper 1986, 32, 110.
17. Turng, L. S.; Wang, K. K. ASME J Eng Ind 1990, 112, 161.
18. Chen, S. C.; Chung, Y. C. Int Comm Heat Mass Transfer 1992, 19, 559.
19. Himasekhar, K.; Lottey, L.; Wang, K. K. ASME J Eng Ind 1992, 114, 213.
20. Chen, S. C.; Chung, Y. C. ASME J Heat Transfer 1995, 117, 550.
21. Hu, S. Y.; Cheng, N. T.; Chen, S. C. Plast Rubber Compos Pro 1995, 23, 221.
22. Holman, J. P. in Heat Transfer, McGraw-Hill, New York, 1989, p. 274.
23. Brebbia, C. A.; Telles, J. C. F.; Wrobe, L. C. in Boundary Element Technique, Springer-Verlag, New York, 1984, p. 60.
24. Barone, M. R.; Caulk, D. A. J Appl Mech 1985, 35, 311.
25. Rezayat, M.; Burton, T. in Symposium of Advanced Boundary Element Methods: Application in Solid and Fluid Mechanics, Cruse, T. A., Ed., Springer-Verlag, Berlin, 1987.
26. Chen, S. C.; Chung, Y. C. Int Commun Heat Mass Transfer 1994, 21, 323.
27. Chen, S. C.; Hu, S. Y. Int Commun Heat Mass Transfer 1991, 18, 823.